Transformer Core Modelling

Washington L. A. Neves
Universidade Federal da Paraíba (UFPB)
Departamento de Engenharia Elétrica
Av. Aprígio Veloso 822
58 100 Campina Grande - PB - Brazil

Hermann W. Dommel
The University of British Columbia
Department of Electrical Engineering
2356 Main Mall, Vancouver, B.C.
Canada, V6T 1Z4

Abstract

In this paper, a general discussion of hysteresis and eddy losses in iron core is presented. RL networks, in which the inductances are nonlinear and the resistances are linear, are developed to model the nonlinear and frequency-dependent effects of the transformer core (saturation, eddy currents and hysteresis). It is assumed that the core loss is known as a function of frequency. Simulations are compared to laboratory measurement of inrush current and to a ferroresonance field test. The developed model is compared to simpler core models as well.

1 Introduction

Rosales and Alvarado[1] represented eddy current effects in the core by solving Maxwell's equations within the laminations assuming that the permeability and conductivity of the material were constant. They derived expressions for the lamination impedance $Z_l(j\omega)$ and admittance $Y_l(j\omega)$ in the forms:

$$Z_l(j\omega) = R_l \xi \tanh(\xi), \qquad (1)$$

and

$$Y_l(j\omega) = (1/R_l\xi)\coth(\xi) \qquad (2)$$

for

$$R_l = \frac{2w}{\sigma l d} \quad \text{and} \quad \xi = d\sqrt{j\omega\mu\sigma},$$

where l is the lamination length; w the lamination width; $2d$ the lamination thickness; μ the magnetic permeability of the material and σ the electric conductivity of the lamination.

From the expansion of the hyperbolic tangent in (1) into partial fractions

$$\tanh\xi = 2\xi\sum_{k=1}^{\infty}\frac{1}{\xi^2+\left[\pi(2k-1)/2\right]^2}, \qquad (3)$$

they realized a series Foster-like linear circuit and from the expansion of the hyperbolic cotangent, they realized the parallel Foster-like circuit of Figure 1. The accuracy of the representation depends on the number of terms retained in the partial fraction expansion.

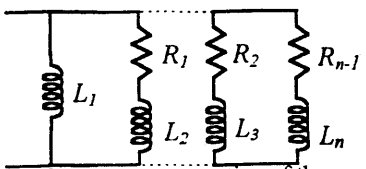

Figure 1: Eddy Current representation of the core after [1]

Tarasiewicz et al.[2] used (1) and expanded the hyperbolic tangent in continued fraction form,

$$\tanh\xi = \cfrac{\xi}{1+\cfrac{\xi^2}{3+\cfrac{\xi^2}{5+\cfrac{\xi^2}{7+\cfrac{\xi^2}{9+\cdots}}}}} \qquad (4)$$

and realized the ladder network of Figure 2a, known as the standard Cauer circuit.

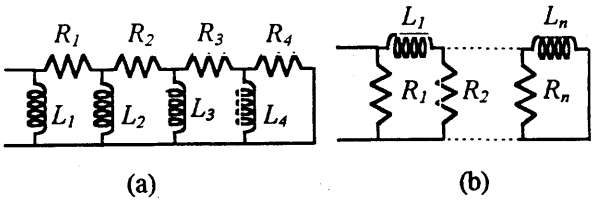

Figure 2: a)Eddy Current representation of the core after [2]
b) Eddy Current representation of the core after [4]

They observed that the number of terms to be retained in the continued fraction of (4) is smaller than the number of terms to be retained in the partial fraction of (3) for the same frequency range and verified that the four sections of the continued fraction model of Figure 2a would be enough to reproduce the exact impedance of (1) for a frequency range up to 200kHz with an error less than 5%. They also noticed that to achieve the same accuracy, 72 sections of the Foster-like circuit of Figure 1 would be required. Based on that, they decided to work with the standard Cauer circuit. However, it seems the authors were not aware that once the circuit parameters of Figure 2a are known, a Foster-like equivalent circuit which reproduces the same frequency response with exactly the same number of elements can be realized as well (later on, network realizations will be addressed)[3]. Therefore, it seems there is no apparent gain in choosing this ladder network to represent eddy current effects in the core.

De Leon and Semlyen[4] suggested the Cauer circuit of Figure 2b. The RL parameters were obtained by a nonlinear fitting process to match (1). This circuit can be interpreted as a discretization of the lamination. The inductances represents the flux paths and the resistances produce the eddy loss. At DC excitation, the current flows through the magnetizing inductances lying longitudinally (in the previous circuits, the DC current flows through one inductance only). This could be interpreted as a uniform flux distribution in the entire lamination at DC level.

3 Core Loss

A more detailed core model should take into account the nonlinear and frequency-dependent effects of saturation, hysteresis and eddy currents. It should be emphasized that information about how eddy and hysteresis losses are split, is in fact artificial. Today, the point of view of many researchers is that virtually all the observed losses are resistive losses associated with micro eddy currents due to Barkhausen jumps of domain walls [5,6], no matter how slow the magnetization loops are traversed.

Core models in which hysteresis and eddy currents are treated simultaneously are developed in the next sections. A Foster-like circuit is used to represent both, hysteresis and eddy current effects. First, consideration is given to the core operating in the linear region. Nonlinear effects are considered later.

4 Eddy Current and Hysteresis Modelling

There is a property of linear passive networks in which the knowledge of the real part of an impedance Z(s) for s=jω (Re (Z(jω)), completely determines Z(s) [7]. If (Re (Z(jω)) is a given rational function of frequency ω, then one can construct the corresponding rational function Z(s) in terms of the complex frequency variable s. Once Z(s) is known, it can be realized as a passive network [3,7,8]. The same process applies to the admittance function Y(s), as described next.

4.1 Construction of Y(s) from Its Real Part

The process of constructing Y(s) or Z(s) from their real parts is well known in network synthesis theory and only a brief discussion is presented here. For more details, the reader is referred to [3,7].

Consider first a simple circuit composed of only two linear RL elements connected in parallel (Figure 4a).

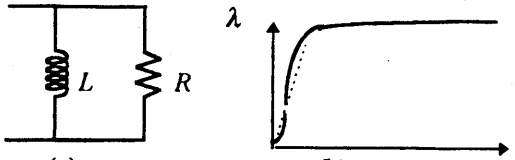

Figure 3: Core parameters.

Its admittance Y(s) could be written in the form

$$Y(s)=\frac{1}{R}+\frac{1}{sL}.$$

It follows that

$$G=1/R=(Y(s)+Y(-s))/2. \qquad (5)$$

If the elements are frequency-dependent, $G(\omega)=1/R(\omega)=\mathrm{Re}[Y(j\omega)]$, or with s=jω,

$$\mathrm{Re}[Y(s)]=(Y(s)+Y(-s))/2. \qquad (6)$$

Now, consider the exciting branch of a single-phase transformer to be linear (the extension of the method to include saturation effects will be done later). One can visualize the core operating below the knee of the saturation curve. In this region, the saturation curve could be approximated by a linear segment (dashed line of Figure 3b). The exciting branch can be represented by a frequency-dependent lossy element R(ω) in parallel with the magnetizing inductance L(ω). The relation which ties R(ω) to L(ω) is shown below.

First represent Y(s) as a rational function containing n pairs of poles and zeroes :

$$Y(s)=\frac{N(s)}{D(s)}=K_\infty\frac{(s+z_1)(s+z_2)\cdots(s+z_n)}{(s+p_1)(s+p_2)\cdots(s+p_n)}, \qquad (7)$$

p_i and z_i are real and positive, i.e., the poles and zeroes of Y(s) lie on the left hand side of the s plane. From (6) and (7), the real part of Y(s) is expressed by:

$$\mathrm{Re}[Y(s)]=\frac{1}{2}\left[\frac{N(s)D(-s)+N(-s)D(s)}{D(s)D(-s)}\right]$$

or

$$\mathrm{Re}[Y(s)]=\frac{U(s^2)}{W(s^2)}=K_\infty\frac{(-s^2+u_1^2)\cdots(-s^2+u_n^2)}{(-s^2+p_1^2)\cdots(-s^2+p_n^2)}, \qquad (8)$$

where u_i is also positive and real [9]. Expanding (8) into partial fractions

$$\mathrm{Re}[Y(s)]=K_\infty+\frac{K_1}{(-s^2+p_1^2)}+\cdots+\frac{K_n}{(-s^2+p_n^2)}. \qquad (9)$$

Further expanding each fraction of the equation above into two partial fractions

$$\mathrm{Re}[Y(s)]=K_\infty+\frac{K_1/2p_1}{(-s+p_1)}+\frac{K_1/2p_1}{(s+p_1)}+\cdots+\frac{K_n/2p_n}{(s+p_n)}+\frac{K_n/2p_n}{(-s+p_n)}$$

or

$$\mathrm{Re}[Y(s)]=\left(\frac{K_\infty}{2}+\cdots+\frac{K_n/2p_n}{(s+p_n)}\right)+\cdots+\left(\frac{K_\infty}{2}+\cdots+\frac{K_n/2p_n}{(-s+p_n)}\right). \qquad (10)$$

Comparing (6) and (10) it is clear that the admittance function is given by:

$$Y(s)=K_\infty+\frac{K_1/p_1}{(s+p_1)}+\frac{K_2/p_2}{(s+p_2)}+\cdots+\frac{K_n/p_n}{(s+p_n)} \qquad (11)$$

From (11), one can also write the admittance in the form:

$$Y(s)=\frac{a_ns^n+\cdots+a_2s^2+a_1s+a_0}{b_ns^n+\cdots+b_2s^2+b_1s+b_0} \qquad (12)$$

It can be seen that if the function G(ω)=Re[$Y(j\omega)$] is known, $Y(s)$ is determined.[1] It should be pointed out that G(ω) must be expressed as an even rational function in ω^2 with real coefficients in the form of (8) with $\omega^2=-s^2$ and $0\le G(\omega)<\infty$ for all frequencies [7]. A curve fitting procedure to obtain G(ω) or R(ω) in the required form, from one of the core loss - frequency curves supplied by steel lamination manufacturers, is explained in Appendix A. It is recommended that the data be taken for an induction level, at which the lamination is not saturated.

4.2 Linear Network Synthesis

From Y(s), any of the RL equivalent networks of Figure 4 can be realized with the same minimum number of elements. If for any of these circuit, the parameters are known, Y(s) or Z(s)=1/Y(s) could be determined and the remaining circuits could be realized as well. It must be

[1] The construction of Y(s) from its real part in the partial fraction form of (11) was first suggested by Bode[9]. There is a method to compute the coefficients a_i and b_i in (12) directly from (8) due to C.M. Gerwetz [3]

clear that all these circuits are equivalents only with respect to their terminals, i.e., the network elements of each circuit must have the proper values to produce the same terminal impedance or admittance as a function of the complex frequency s.

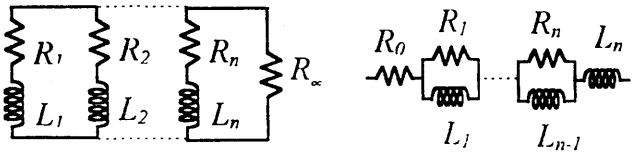

a)Parallel RL Foster network b) Series RL Foster network

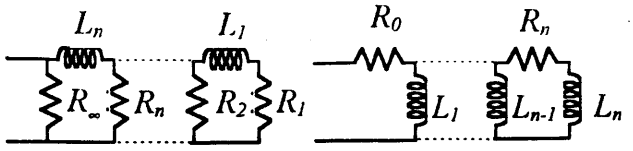

c) Physical Cauer network d) Standard Cauer network

Figure 4: Realization of RL networks.

Let us describe the algebraic process for realizing the parallel Foster-like circuit. The terminal admittance of the RL network of Figure 4a is

$$Y(s)=\frac{1}{R_\infty}+\sum_{i=1}^{n}\frac{1/L_i}{s+R_i/L_i}. \qquad (13)$$

This circuit could be realized directly from (11) with

$$R_\infty=\frac{1}{K_\infty},\quad L_i=\frac{p_i}{K_i}\quad \text{and}\quad R_i=\frac{p_i^2}{K_i}.$$

For the Cauer circuit of Figure 4c Y(s) is written in the continued fraction form:

$$Y(s)=\frac{1}{R_\infty}+\cfrac{1}{L_n s+\cfrac{1}{\cfrac{1}{R_n}+\cfrac{1}{L_{n-1}s+\cdots+\cfrac{1}{\cfrac{1}{R_2}+\cfrac{1}{L_1 s+R_1}}}}}. \qquad (14)$$

Equation (14) could be derived from (12) according to the following steps:

a - from (12) Y(s) is split into two terms by removing the constant a_n/b_n;

$$Y(s)=\frac{a_n}{b_n}+\frac{a'_{n-1}s^{n-1}+\cdots+a'_2s^2+a'_1s+a'_0}{b_ns^n+\cdots+b_2s^2+b_1s+b_0} \qquad (15)$$

or

$$Y(s)=\frac{a_n}{b_n}+\cfrac{1}{\cfrac{b_ns^n+\cdots+b_2s^2+b_1s+b_0}{a'_{n-1}s^{n-1}+\cdots+a'_2s^2+a'_1s+a'_0}}$$

b - removing $\frac{b_n}{a'_{n-1}}s$ from the denominator of the second term of the equation above, results

$$Y(s)=\frac{a_n}{b_n}+\cfrac{1}{\cfrac{b_ns}{a'_{n-1}}+\cfrac{1}{\left[\cfrac{a'_{n-1}s^{n-1}+\cdots+a'_2s^2+a'_1s+a'_0}{b'_{n-1}s^{n-1}+\cdots+b'_2s^2+b'_1s+b'_0}\right]}}. \qquad (16)$$

Now, the process of long division is done for the term between the brackets (steps a and b are repeated). For each cycle, a constant (step a) and a pole at s=∞(step b) are removed. The process continues until the order of the polynomial in the last continued fraction is one. For the remaining circuit realizations of Figure 5, the reader is referred to [3].

A remark must be made about the calculation of Y(s). Consider the Foster-like circuit of Figure 4a with an inductance L_{dc} placed across its terminals (Figure 5). It is clear that L_{dc} does not affect the conductance G(ω); it affects only the susceptance. In the process described earlier, Y(s) is the minimum admittance function that produces G(ω). The full admittance is given by L_{dc} in parallel with Y(s).

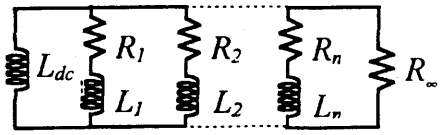

Figure 5: Frequency-dependent representation of the core.

4.3 Iron Core Nonlinearities

Since the resistances and inductances in the circuit of Figure 5 do not represent any physical part of the core, it is not clear how to incorporate nonlinear effects. Considering that low frequency elements contribute more to saturation than high frequency elements, only the inductance L_{dc} is made nonlinear. The Foster-like circuit was chosen because it has only two nodes, therefore, it is computationally more efficient than the remaining circuits of Figure 4.

4.4 Numerical Example - Hysteresis

It is appropriate to illustrate how the model works for an example in which a core is assumed to experience only hysteresis loss (this is an arbitrary case since hysteresis and eddy losses cannot be separated). Initially, suppose hysteresis could be reproduced by a resistance in parallel with a nonlinear inductance. For a sinusoidal applied voltage, at rated frequency, the flux-current loop of Figure 6a is obtained. Let us keep the flux amplitude constant.[2] For any frequency, the area inside the flux-current loops should be the same and the loss is a function of how fast the trajectories are traversed. For a frequency equal to twice the rated frequency, the voltage doubles. So, hysteresis resistance would have to be twice the hysteresis resistance at rated frequency to produce the same loss per cycle. For any frequency, the resistance R_r should be replaced by an equivalent frequency-dependent resistance $R(\omega)$ according to:

$$R(\omega)=R_r\omega/\omega_r, \qquad (17)$$

where ω_r is the rated angular frequency and R_r is the hysteresis resistance at rated frequency.

Let us now represent the core by a two slope λ-*i* curve, defined by points in Table 1, and a resistance R_r=100 Ω at rated frequency (60Hz). Using the method described in

[2] This could be acomplished by keeping constant the ratio between the amplitude of the voltage signal and the frequency.

the previous sections with $W_h >> W_{eddy}$ (Appendix A), the Foster-like circuit parameters of Figure 4a are found for a frequency range from 60 Hz to 3 kHz. The fitted frequency-dependent resistance and its value from (17) are shown in Figure 6b.

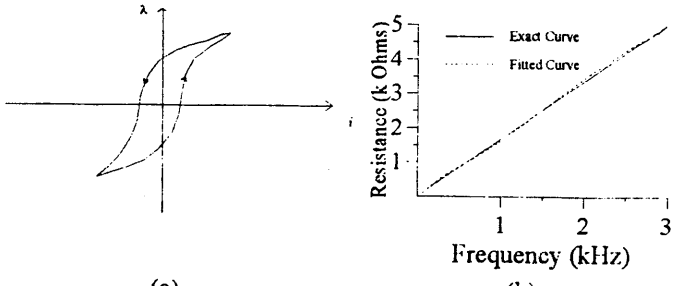

(a) (b)

Figure 6 : a) $\lambda - i$ hysteresis curve.
b)frequency-dependent resistance

Table 5.1 : Flux-current curve

Current (A)	Flux (V.s)
0.0000	0.0000
20.0000	0.4000
300.0000	0.6000

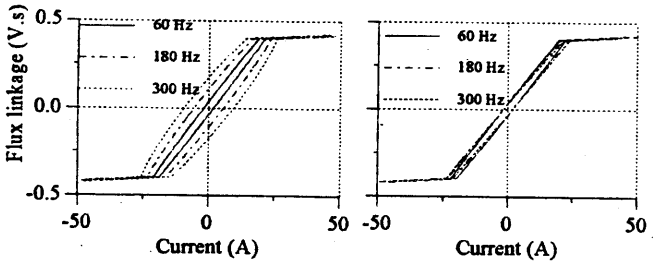

(a) (b)

Figure 7: a) Constant resistance.
b) Frequency-dependent resistance

The flux-current plots shown in Figure 7 were obtained from time-domain simulations using Microtran®[10]. Sinusoidal flux linkages of constant amplitudes and frequencies of 60 Hz, 180 Hz and 300 Hz, were used for the simulations. In Figure 7a, the loops were obtained considering the core loss represented by a constant resistance and, in Figure 7b, with the frequency-dependent model developed here. In Figure 7b, the area of the loops are nearly independent of the frequency, however, the flux-current loops tilt slightly clockwise as frequency increases. In a qualitative way, one could interpret that an increase of the core resistance is associated with a decrease in the core inductance caused by the flux being pushed away from the center of the lamination.

5 Inrush Current

A single-phase 60 Hz, 1 kVA , 208/104/120 V laboratory transformer, in which the core is made of non-oriented silicon steel laminations, was tested. From short-circuit tests, with the voltage source connected to the 104 V side:

1. AC resistance measured with the 120V side short-circuited - 0.60 Ω;

2. Leakage reactance with the 120 V side short circuited - 0.19 Ω;

3. DC winding resistance - 0.40 Ω.

The points (empty circles) of the flux-current characteristic of Figure 8a were obtained from no-load loss measurements and V_{rms}-I_{rms} values, using the method developed in Chapter 3 of [12]. When the core is operating in the unsaturated region, its inductance can be roughly approximated by 2.4 H. The core loss at 60 Hz is represented by a constant resistance of 1.8 k Ω. All parameters are referred to the 104 V terminal.

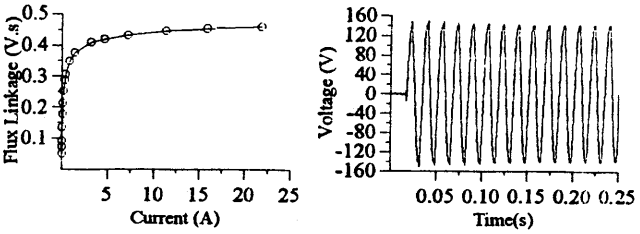

(a) (b)

Figure 8: a)Flux-current curve; b) Input voltage.

The Foster-like circuit linear parameters shown in Table 2, was calculated for a frequency range from 60 Hz to 3 kHz assuming the ratio of hysteresis to eddy loss per cycle to be W_h/W_{eddy}=2 at 60 Hz [11] (it does not make any difference in the simulations if this ratio is taken as 1 or 3). The transformer was initially demagnetized and later, a voltage source was switched in the 104 V terminal. The voltage signal (Figure 8b) was saved as an ASCII file and used as input in Microtran®. The inrush current waveform was measured as well. Plots of the simulated current using two core models (Foster-like circuit and a constant resistance in parallel with a nonlinear inductance) and the measured current using a time step of 50 μs, are shown in Figure 9a. For the study, a straight line segment was connected to the last point of the curve of Figure 8a. Its slope was chosen to match the first peak of the measured current, when the flux linkage reached its first peak (the flux waveform was obtained integrating the voltage waveform of Figure 8b).[3]

Table 5.2: Linear circuit parameters

Foster-like circuit parameters	
L_{dc}= 2.4000 H	R_1= 1722.4899 Ω
L_1 = 4.1518 H	R_2= 22264.6946 Ω
L_2= 4.6595 H	R_∞= 5271.3702 Ω

In general, the agreement between measurement and simulations, for any of the used models, is good. Figure 9b is a magnification of Figure 9a for the time interval between 0.15 and 0.20s. The two core models produce nearly the same response and are in good agreement with measurements. Another simulation was performed

[3] By extending the last segment of Figure 8a, it was found that the first current peak in the simulations was underestimated by nearly 5%. The winding resistance, used for the simulations, was 0.45 Ω which is slightly above the measured value.

representing the core by a nonlinear inductance only. The current waveform was nearly the same as the constant resistance curve of Figure 9.

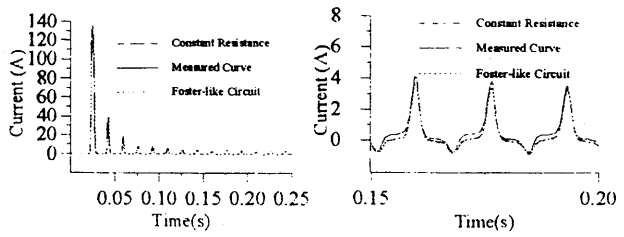

Figure 9: Transformer inrush current.

6 Ferroresonance

Consider the BPA (Bonneville Power Administration) 1100kV test system (details in [12]). It comprises a generating station, a transformer bank (autotransformers) and a short three-phase transmission line. Field tests were carried out. Ferroresonance occurred in phase A when this phase was switched off on the low voltage side of the transformer. The transformer exciting branch is represented by a Foster-like circuit with the parameters calculated for a frequency range from 60 Hz to 3 kHz, assuming the ratio of hysteresis to eddy loss per cycle to be $W_h/W_{eddy}=1$ at 60 Hz [13]. The simulation and field test results for the voltage at phase A (transformer high voltage terminal), are shown in Figure 10.

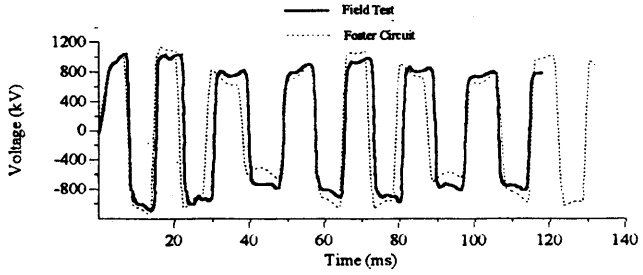

Figure 10: Ferroresonance in a power system.

The Foster-like circuit produces nearly the same response as a linear resistance in parallel with a nonlinear inductance.

5.7 Summary

An approach to model frequency-dependent effects in the transformer core from core loss data was presented. The parallel Foster-like circuit model, in which hysteresis and eddy current effects are treated simultaneously, was realized. Theoretically, the circuit models can be used for any frequency range (minimum frequency must not be zero).

If the circuit model is used to represent a core in which the hysteresis loss is dominant (e.g. amorphous core [14]), the core loss per cycle is nearly independent of the frequency. The flux-current trajectories are generated by the circuit models with no need to pre-define them.

An inrush current case and a ferroresonance case were used as test examples. For both cases, there were no major improvements in representing frequency-dependent effects in the core.

It is still premature to say that frequency-dependent effects in the core are not important for all transient cases. More validation tests against other field measurements need to be made in the future, to fully determine their importance for practical applications.

References

1. J. Avila-Rosales and F. L. Alvarado, Nonlinear Frequency Dependent Model for Electromagnetic Transient Studies in Power Systems , IEEE Trans. Power App. Syst. vol. PAS-101, Nov. 1982, pp. 4281-4288.
2. E.J. Tarasiewicz, A. S. Morched, A. Narang and E. P. Dick, *Frequency Dependent Eddy Current Models for Nonlinear Iron Cores*, IEEE Transactions on Power Systems, Vol. 8, No. 2, May 1993, pp.588-597.
3. Ernst A. Guillemin, *Synthesis of Passive Networks*, Chapter 8, John Wiley & Sons Inc., New York, 1957.
4. F. De Leon and A. Semlyen, *Time Domain Modeling of Eddy current Effects for Transformer Transients*, IEEE Transactions on Power Delivery, Vol. 8, No. 1, January 1993, pp.271-280.
5. B. D. Cullity, *Introduction to Magnetic Materials*, Addison Wesley Publishing Company, 1972.
6. J. J. Becker, *Magnetization Changes and Losses in Conducting Ferromagnetic Materials*, Journal of Applied Physics, Vol. 34, No. 04 (Part 2), April, 1963, pp. 1327-1332.
7. David F. Tuttle, *Electric Networks Analysis ant Synthesis*, Chapter XI, McGraw Hill Inc. 1965.
8. Jiri Vlach, *Computerized Approximation and Synthesis of Linear Networks*, Chapter IV, John Wiley & Sons Inc., New York, 1969.
9. Athanasios Papoulis, *The Fourier Integral and Its Applications*, McGraw Hill Book Company Inc.,1962, pp.195-196.
10. Microtran Power System Analysis Corporation, *Transient Analysis Program Reference Manual*, Vancouver, Canada, 1991.
11. United States Steel, *Electrical Steel Sheets Engineering Manual*, 4th Edition, 525 William Penn Place, Pittsburgh 30, PA.
12. Washington. L. A. Neves, *Transformer Modelling for Transient Studies*, Chapter 2, Ph. D. Thesis, The University of British Columbia, December 1994.
13. A. C. Franklin and D. P. Franklin, *The J & P Transformer Book: A Practical Technology of the Power Transformer*, 11th Edition, Butterworths, 1983.
14. G. E. Fish, *Soft Magnetic Materials*, Proceedings of the IEEE, Vol. 78, No. 6, June 1990, pp. 947-972.
15. William H. Press, Saul A. Telkolsky, William T. Vetterling, Brian P. Flannery, *Numerical Recipes, The Art of Scientific Computing*, 2nd Edition, Section 5.13, Cambridge University Press, New York,1992.

Appendix A-Rational Approximation of the Real Part of Y(s)

A.1 Fitting Procedure

Similar to equation (8), the frequency-dependent resistance could be expressed as rational function in $-s^2$

$$R(s)=R_\infty\frac{(-s^2+a_1^2)(-s^2+a_2^2)\cdots(-s^2+a_n^2)}{(-s^2+b_1^2)(-s^2+b_2^2)\cdots(-s^2+b_n^2)} \qquad (A.1)$$

and with s=jω, R(ω) is written in the form:

$$R(\omega)=K_c\frac{(c_1\omega^2+1)(c_2\omega^2+1)\cdots(c_n\omega^2+1)}{(d_1\omega^2+1)(d_2\omega^2+1)\cdots(d_n\omega^2+1)} \qquad (A.2)$$

Where K_c, $c_i=1/a_i^2$ and $d_i=1/b_i^2$ are positive real numbers, with $i=1,2,\cdots,n$.The right hand side of (A.2) is fitted to the known function R(ω). The goal here is to compute K_c, c_i and d_i. The number of terms n will depend on the frequency range of interest. R(ω) is fitted interval by interval as shown in Figure A.1 starting with the interval between ω_{min} and ω_1 and ending with the interval between ω_n and ω_{max} .

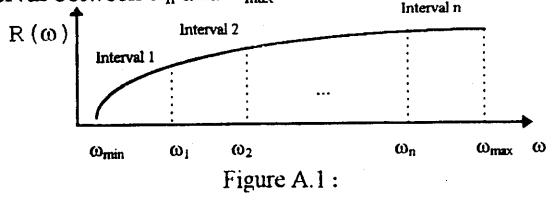

Figure A.1 :

The algorithm proceeds as follows:

1 - For interval 1, write R(ω) as

$$R(\omega) = K_c \frac{(c_1\omega^2 + 1)}{(d_1\omega^2 + 1)} = \frac{K_d\omega^2 + K_c}{(d_1\omega^2 + 1)}$$

or $$K_d\omega^2 - d_1 R(\omega)\omega^2 + K_c = R(\omega) \qquad (A.3)$$

2 - Estimate ω_1. Take m frequency sample points between ω_1 and ω_{min}. Build the overdetermined system of equations (A.3) with only the parameters K_c, K_d and d_i unknown. A weighted linear least square fitting routine[15] is used to find these parameters ($c_1 = K_d/K_c$ is also computed). If the maximum error in the fitting is less than a predifined value, proceed to next step, If not, ω_1 is reduced by small steps $\Delta\omega_1$ and the system of equations (A.2) is reevaluated.

3- For interval 2 in Figure A.1, write R(ω) as

$$R(\omega) = K_c \frac{(c_1\omega^2 + 1)(c_2\omega^2 + 1)}{(d_1\omega^2 + 1)(d_2\omega^2 + 1)},$$

with K_c, c_1 and d_i already known from the previous step. Estimate ω_2 and find c_2 and d_2 following the procedure of step 2, with the m frequency samples now taken between ω_{min} and ω_2.

For the remaining intervals in Figure A.1, c_i and d_i are found in the same fashion and the constants R_∞, a_i and b_i of (A.1) are determined.

Experience has shown that a first estimate of $\omega_1 = 5\omega_{min}$ (with $\Delta\omega_1 = 0.1\omega_{min}$) and subsequent estimates of $\omega_{i+1} = 10\,\omega_i$ (with $\Delta\omega_i = 0.1\omega_{i-1}$ for $i \geq 2$) are usually very close to the final values for an error of 3% and 100 frequency samples used as input parameters to the fitting routine.

A.2 G(ω) Obtained from Lamination Data

Steel manufacturers may supply core loss vs. frequency curves for the most commom lamination grades subjected to constant flux amplitudes[4]. These data are generally obtained on Epstein samples using a sine wave voltage source following the test procedure of ASTM Standard Method A-34. With this information one can obtain either the frequency-dependent resistance R(ω) or conductance G(ω) as described next.

In the sinusoidal steady state the average power P_{loss} is:

$$P_{loss} = P(\omega). \qquad (A.4)$$

R(ω) is obtained by: $R(\omega) = V_m^2 / (2P_{loss}) = \lambda_m^2\omega^2 / (2P(\omega))$,

where V_m and λ_m are the amplitude of the applied voltage and flux, respectively. Since the flux is kept constant, R(ω) can be written as

$$R(\omega) = K\omega^2 / P(\omega). \qquad (A.5)$$

It is convenient to normalize R(ω) assuming that the resistance measured at the transformer rated frequency ω_r is $R(\omega_r)=1$. So, the constant K in the equation above is

$$K = P(\omega_r) / \omega_r^2. \qquad (A.6)$$

and the normalized resistance $R_N(\omega)$ is

$$R_N(\omega) = P(\omega_r)\omega^2 / (\omega_r^2 P(\omega)). \qquad (A.7)$$

So, if the transformer lamination loss vs. frequency curve is known, an estimate of the frequency-dependent core loss resistance can be made by scaling the normalized resistance $R_N(\omega)$ to the resistance at rated frequency $R(\omega_r)$. Then, $R(\omega) = R_N(\omega)\cdot R(\omega_r)$, and $G(\omega) = 1/R(\omega)$.

A.3 G(ω) Obtained from Standard Tests

The frequency-dependent core resistance could also be estimated from transformer standard tests. The plot of loss/cycle can be crudelly approximated by a straight line, as shown in Figure A.2.

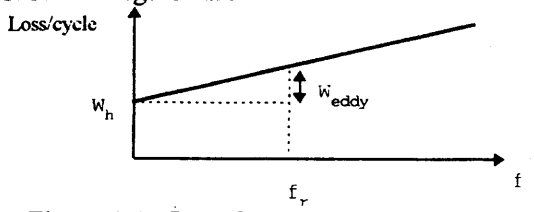

Figure A.2 : Transformer core loss curve at rated

Power transformer manufacturers usually supply two or three values of no-load loss at different frequencies, with the flux kept at the rated level. From Figure A.2, the loss per cycle coud be written as

$$\frac{P_{loss}}{f} = W_h + W_{eddy}\cdot\frac{f}{f_r}, \qquad (A.8)$$

where f is the frequency in which the loss is measured, f_r is the rated frequency, W_h is the hysteresis loss per cycle and W_{eddy} is eddy loss per cycle at the rated frequency.

Taking (A.8) and writing the loss for the angular frequency $\omega = 2\pi f$,

$$P_{loss} = \frac{1}{2\pi}\left(W_h\cdot\omega + W_{eddy}\cdot\frac{\omega^2}{\omega_r}\right). \qquad (A.9)$$

From (A.5) and (A.9), the resistance R(ω) is

$$R(\omega) = \frac{\lambda_m^2\omega^2}{2P_{loss}} = \frac{\lambda_m^2\omega^2}{\frac{1}{\pi}\left(W_h\cdot\omega + W_{eddy}\cdot\frac{\omega^2}{\omega_r}\right)} \qquad (A.10)$$

Normalizing R(ω), as done for (A.6) and (A.7),

$$R_N(\omega) = K\omega / (ratio + \omega/\omega_r), \qquad (A.11)$$

where ratio=W_h/W_{eddy} and $K = (ratio+1)/\omega_r$.

The resistance and conductance are then:

$$R(\omega) = R_N(\omega)\cdot R(\omega_r), \text{ and } G(\omega) = 1/R(\omega). \qquad (A.12)$$

If the transformer manufacturer does not supply the core loss vs. frequency curve, a typical ratio W_h/W_{eddy} is commonly taken as unity [13]. In practice, the straight line of Figure A.2 could be drawn using loss measurement data gathered from routine tests. For instance, it could be obtained from the loss measurement taken at rated voltage and rated frequency and, as recommended by ANSI C57.12.90 (Induced Overvoltage Withstand Test), from the loss measurement taken at twice the rated frequency and double voltage amplitude.

[4] To avoid confusion of trade names, the American Iron and Steel Institute has assigned AISI type numbers to electrical steel. These consist of the letter "M" (for magnetic material) followed by a number which, when the designations were originally made, was about to ten times the core loss in watt/lb at 15 kilogauss (1.5 T) and 60 Hz for 29 gage sheet (0.0140 in). Core losses have since been reduced but the type numbers remain [5].